IPS Journal of Molecular Docking Simulations
IPS J Mol Dock Sim., 2(1): 12-24 (2023)
DOI: https://doi.org/10.54117/ijmds.v2i1.18

In silico and *In vivo* Studies of *Calotropis procera* Leaf and Root Extracts on Mitochondrial-Related Parameters in Wistar Rats

Ayobami Damilare Adisa[1], Patience Folashade Olabinri[1], Adejoke Tolulope Oyedeji[2], Fiyinfoluwa Demilade Ojeniyi[1], James Agboola[3], Muinat Fehintola Zubair[1], Gbadebo Joshua Ojo[1], Leonard Ona Ehigie[1], Adeola Folasade Ehigie[1*]

[1]Department of Biochemistry, Ladoke Akintola University of Technology, Ogbomoso, Nigeria.
[2]Department of Biochemistry, University of Lagos, Lagos, Nigeria
[3]Department of Biochemistry, Obafemi Awolowo University Ile-Ife, Nigeria

Author email: afehigie@lautech.edu.ng

Abstract

Drugs targeting Mitochondrial Membrane Permeability Transition (MMPT) pore opening are of great interest for conditions arising from apoptosis dysregulation. This study investigate MMPT pore inducing effect of *Calotropis procera* leaves and root extracts on mitochondrial-related parameters in the liver of healthy male Wistar rats. Extraction was done by standard methods, using Ethylacetate and Butanol solvent. Fifty–two rats weighing between 130 g - 150 g were divided into thirteen groups (n=4). Group 1 received distilled water, other groups were administered ethylacetate leaf extract (ELE), butanol leaf extract (BLE), ethylacetate root extract (ERE) and butanol root extracts (BRE). Liver Mitochondrial pore opening, mitochondrial ATPase activity and lipid peroxidation were assessed spectrophotometrically, while the interaction between human Cyclophilin D (a pore activating protein with PDB ID: 2BIT) and identified phytochemicals of *C. procera* leaves and roots extracts were studied *In-silico*. Varying concentrations of the extracts induced MMPT pore opening by 6.6, 7.4 and 5.9 folds for BLE and 10.2, 7.3 and 6.4 folds for ELE at 40, 50 and 60 mg/100g bw respectively when compared with control group. Root extracts showed significant MMPT pore opening with a fold increase of 12.2, 10.1 and 20.4 for BRE and 11.37, 11.84, for ERE at at 40 , 50 and 60 mg/100g bw respectively. BLE, BRE, ELE and ERE showed increase in ATPase activities with respect to the control group. Malondialdehyde (MDA) levels as an indication of lipid peroxidation increased significantly when compared with control. Molecular docking and simulation showed the existence of stable interactions between human Cyclophilin D with phytochemicals of *C. procera* with 2"-Oxovoruscharin having highest binding affinity of -7.9 kcal/mol. *C. procera* has potential for therapeutic use for the treatment of disorders related to derangement of apoptosis.

Keywords: *2"-Oxovoruscharin; Cyclophilin D; Molecular Simulation; Mitochondrial swelling; Atpase; Malondialdehyde; Calotropis procera*

Article History

Received: 22 May 2023
Accepted: 26 Jul 2023
Published: 03 Sept 2023

Scan QR code to view♦

How to cite this paper: Adisa, A. D., Olabinri, P. F., Oyedeji, A. T., Ojeniyi, F. D., Agboola, J., Zubair, M. F., Ojo, G. J., Ehigie, L. O., & Ehigie, A. F. (2023). In silico and In vivo Studies of Calotropis procera leaf and root extracts on Mitochondrial-Related parameters in Wistar Rats. *IPS Journal of Molecular Docking Simulations, 2*(1), 12–24. https://doi.org/10.54117/ijmds.v2i1.18.

Introduction

Mitochondria are essential for human survival because they are involved in a number of energy-dependent biological processes such as cell growth, cell messaging, aging, and replication. As a result, mitochondria have been linked to a number of diseases affecting energy-dependent organs and tissues such as the heart, brain, and skeletal muscle (Schardt, 2008). Since electron transport and proton leakage influence mitochondrial membrane potential (or proton motive force), it is the fundamental bio-energetic parameter governing respiratory rate, ATP synthesis, and reactive oxygen species generation (Nicholls, 1974a). The opening of the mitochondrial membrane permeability transition (MMPT) channel induces the release of apoptotic proteins, hence initiating apoptosis (Ling *et al.*, 2010). Dissipation of mitochondrial trans-membrane potential (m) and ATP synthesis are caused by an abrupt and irreversible increase in the permeability of the inner mitochondrial membrane (IMM) to tiny solutes. "mitochondrial membrane permeability transition" refers to the osmotic disintegration of the

mitochondrial organelle and the uncontrolled entry of water into the mitochondrial matrix (Bonora *et al.*, 2015).

The MMPT Pore may function as a self-amplifying "switch" that irreversibly condemns the cell to apoptosis when it is activated (Bernarrdi *et al.*, 1994; Zorati and Szabo, 1995). In reaction to high neuronal activity or acute energy shortage, mitochondrial Ca^{2+} overload causes the opening of a nonspecific pore in the inner membrane (Zorati and Szabo, 1995). Ca^{2+}-dependent formation of the MMPT Pore, which represents a rapid increase in permeability to normally impermeable to the inner membrane (Mw 1500 Da) solutes, results in osmotic swelling, membrane rupture, and loss of mitochondrial proteins (Liu *et al.*,1991). The cell exhibits apoptotic characteristics when the mitochondrial membrane permeability transition (MMPT) pore is opened, by activating the release of apoptotic proteins (Ling *et al.*, 2010). Apoptosis in cells is primarily mediated by two well-known pathways (Lockshin and Zakeri, 2004): the extrinsic, or death receptor-mediated, pathway and the intrinsic, or mitochondrial-mediated, pathway (Danial and Korsmeyer 2004). Changes in mitochondrial polarization and the release of apoptogenic mitochondrial proteins result in the activation of caspase-9 and the subsequent cleavage of caspases 3, 6, or 7 (Reed, 2004), which are defining characteristics of the intrinsic apoptotic pathway. These occurrences may start caspase activation and apoptosis (Sun *et al.*, 2004). And surprisingly, various plants have been found to control the mitochondrial permeability transition pore (Ajayi *et al.*, 2016).

Cyclophilin D (CypD) is a highly conserved peptidyl-prolyl cis-trans isomerase (PPIase) that plays an important role in mitochondrial biology. It is produced by the mitochondrial targeting region of the genomic Ppif gene and has a size reduction from 22 to 19 kDa upon entry into the mitochondrial matrix. Its capacity to bind the medication cyclosporine A (CsA), like all cyclophilins, is how it got its name (Walsh *et al.*, 1992). The family of chaperones known as cyclophilins, which has more than 15 members, has been found to accelerate protein folding and maturation in addition to being essential for signal transduction and the immunological response. CypD has been demonstrated to be a sensitizer of the permeability transition pore (PTP), a nonspecific large conductance pore whose opening causes the inner mitochondrial membrane (IMM) potential to dissipate, the loss of ATP production, and ultimately cell death, even though its physiological function is still unknown (Bauer and Murphy, 2020). The PTP has been linked to neurodegenerative diseases (Warne *et al.*, 2016), muscular dystrophies, and ischemia/reperfusion (I/R) injury in the heart (Lim *et al.*, 2011; Bibli *et al.*, 2019), brain (Uchino *et al.*, 2002; Schinzel *et al.*, 2005) and kidney (Park *et al.*, 2011; Yang *et al.*, 2019). The phosphate carrier (PiC) (Leung *et al.*, 2008), the adenine nucleotide translocator (ANT) (Kokoszka *et al.*, 2004; Karch *et al.*, 2019), the F1F0-ATP synthase (Giorgio *et al.*, 2009; Bonora *et al.*, 2017), and the phosphate-binding protein (CypD) have all been Short transient openings of the PTP, however, may play a role in modulating matrix calcium (Petronilli *et al.*, 1999; Bernardi and von Stockum, 2012; Lu *et al.*, 2016; Agarwal *et al.*, 2017), which in turn can control mitochondrial bioenergetics. However, irreversible opening of the PTP is linked to cell death (Elrod *et al.*, 2010; Glancy and Balaban, 2012; Tarasov *et al.*, 2012). Ions, metabolites, lipids, mitochondrial membrane components, soluble proteins, and membrane proteins are only a few of the numerous PTP modulators. In a nutshell, an increase in intramitochondrial calcim, ROS, inorganic phosphate (Pi), and mitochondrial depolarization encourage PTP opening. Physiological PTP antagonists, such as increased levels of mitochondrial membrane potential (m), pH levels above or below the optimal pore-opening pH of 7.3, Mg^{2+}, and adenine nucleotides, especially ADP, counterbalance these influences. CypD controls the PTP, and hence, mitochondrial coupling. It makes PTP more vulnerable to oxidative stress and calcium. Additionally, it has the ability to directly bind to ATP synthase, reducing ATP synthesis whereas CsA's removal of it from the inner mitochondrial membrane promotes ATP synthesis (Giorgio *et al.*, 2009). In mitochondria found in the heart, brain, and liver, CypD controls the assembly of synthasomes (Beutner *et al.*, 2017). Respiration stimulates their production, while their disintegration encourages PTP opening. The synthasomes become more stable when CypD is inhibited or deleted, raising the intriguing possibility that CypD binds to them and prevents their assembly (Beutner *et al.*, 2017). From the information available, it is unclear whether CypD alone is having this effect or if other factors such as matrix calcium levels, redox status, or inner membrane potential are also at play.

Calotropis procera (Aiton) Dryand is a perennial soft-wooded shrub in the Apocynaceae and Asclepiadaceae families (the milkweed family). It's an evergreen xerophytic plant that thrives in dry and semi-arid environments (Al-Rowaily *et al.*, 2020). Calotropis is a Greek word that means "lovely," which alludes to the blossoms, and "procera" is a Latin term that refers to the cuticular wax found on the leaves and stems (Hassan *et al.*, 2015). In different regions of the world, it is known by numerous common names such as apple of Sodom, calotrope, gigantic milkweed, Indian milkweed, wild cotton, rubber tree, ushar, and so on. The fruit morphology of its two subspecies, *C. procera* subsp. procera and *C. procera* subsp. hamiltonii, differs (Dhileepan, 2014). *Calotropis procera* is a multifunctional plant that performs a variety of ecosystem provisioning functions. In North Africa, the Middle East, South Asia, and South-East Asia, it has long been employed in traditional medicinal systems (Al Sulaibi *et al.*, 2020). Since antiquity, it has also been used for fiber, fuel, feed, and lumber (Batool *et al.*, 2020). It has been introduced in numerous places of the world outside of its native range because to its socioeconomic relevance (Asia and Africa). Its naturalization in imported habitats was accomplished by morphophysiological adaptations and the ability to survive a wide range of environmental conditions. As a result, in various locations, the plant has been identified as an invasive weed of wastelands, overgrazed pastures, and poorly managed agricultural fields (Azarpajouh *et al.*, 2021). The Asclepiadaceae family of plants has a wide range of medicinal properties. In traditional medicine, the genus Calotropis is used to treat leprosy, ulcers, tumors, spleen and liver problems, and piles. It also works as a purgative, antihelmintic, anticoagulant, antipyretic, analgesic, antiinflammatory, and antibacterial, as well as a palliative for breathing and blood pressure disorders. It also acts as a neuromuscular blocker

(Jalalpure *et al.*, 2009; Mukherjee *et al.*, 2009; Patra *et al.*, 2009; Seddek *et al.*, 2009). Members of the family are high in cardiac glycosides and are thought to be potential anticancer agents (Barrett & Kieffer, 2001).

Materials and Methods

Plant Material

Calotropis procera roots and leaves were obtained from Ogbomoso, Oyo State, which was identified and authenticated in the Department of plant Biology, LAUTECH, Ogbomoso, Nigeria and voucher number LHO 637 was given. The preparation of *C. procera* roots and leaves extract was done according to the method described by Agbaje and Adeniran, 2009 and modified. Briefly, the fresh roots and leaves of *C. procera* were washed with distilled water, drained and air-dried separately. A known weight of chopped bits (500g) of the air-dried *C. procera* roots and leaves were macerated in 5 L ethylacetate and butanol each for 24 hrs. The macerated mixture was filtered using muslin cloth and the filtrate was collected and taken to rotary evaporator to be concentrated at 40^0C. The obtained moist extract of *C. procera* was freeze dried using a freeze drier. The dried extracts was then orally administered to the male Wistar rats for assessment of their effects on Mitochondrial Membrane Permeability Transition Pore (MMPTP).

Experimental Animal

Fifty-two healthy male Wistar rats weighing between 110g-150g were obtained and kept at the Faculty of Basic Medical Sciences Animal House, Ladoke Akintola University of Technology, Ogbomoso, Nigeria under light controlled conditions (24hrs daily light) and in well-ventilated plastic cages. The rats were randomly allocated into four major groups (n=12) which were further divided into three subgroups. The animals were allowed to acclimatize over a period of two weeks. Each subgroup is fed with 40, 50 and 60 mg/100g bw of Ethylacetate root extract (ERE), Butanol root extract (BRE), Ethylacetate leaf extract (ELE) and Butanol leaf extract (BLE) of *C. procera* respectively for a period of 28 consecutive days. The control animals were fed with distilled water during this period.

Chemicals and Reagents

Sodium Carbonate (Na_2CO_3), Sodium Hydroxide (NaOH), Sodium-Potassium Tartarate (Na-K-C_4O_6), Calcium Chloride ($CaCl_2$), Potassium Hydroxide (KOH), Hydrated Copper Sulphate (CuSO4.5H2O), Methanol were products of BDH Poole UK Ltd. And Co., while Folin Ciocalteau Reagents, BSA, Mannitol, Sucrose, HEPES [4-(2-Hydroxyethyl), EGTA, Spermine, Rotenone, Sodium Succinate were products of Sigma-Aldrich Co, USA. All chemicals were of analytical grade.

Mitochondria Fraction Isolation

According to Lapidus and Sokolove's (1993) and Olorunsogo *et al* (1984), animals were fasted overnight, scarificed by cervical dislocation, and the liver was rapidly excised. This was followed by trimming away any extra tissue and washing the liver in a solution comprising 210 mM Mannitol, 70 mM Sucrose, 5 mM HEPES, 1 M KOH, and 1 mM EGTA, pH 7.4. The liver was then weighed, chopped, and suspended in the same buffer to create a 10% homogenate. It was then homogenized using a Teflon homogenizer. To remove the nuclear fraction and cellular debris, the homogenate was centrifuged twice at 2500 rpm for 5 min in an SM-18B High Speed Refrigerated Centrifuge. The resulting supernatants were centrifuged for 10 minutes at 13000 rpm, and the mitochondrial fractions were then washed three times for 10 minutes at 12000 rpm with a washing buffer that included 210 mM Mannitol, 70 mM Sucrose, 5 mM HEPES-KOH, and 0.5% BSA at a pH 7.4 concentration. The mitochondrial pellets were promptly distributed into 1 ml Eppendorf tubes after being suspended in swelling buffer (210 mM) Mannitol, 70 mM Sucrose, and 5 mM HEPES-KOH, pH 7.4).

Mitochondria Swelling Assay

Mitochondrial permeability transition opening was determined according to the method of Lapidus and Sokolove. Using a Spectrum lab 752ns UV/Visible spectrophotometer, variations in the absorbance of mitochondria at 540 nm in the presence and absence of calcium ions (a triggering agent) were measured. Mitochondria (0.4 mg protein/ml) was incubated for 3 minutes at 30°C in the presence of 8 M rotenone in a medium containing 210 M mannitol, 70 M sucrose, and 5 M HEPES-KOH (pH 7.4). Then, 300 µM $CaCl_2$ was added, followed by the addition of 50 µM sodium succinate, and the MMPT pore opening was measured every 30 seconds for 12 minutes. Spermine's inhibitory effect on the induction of pore opening was also tested. When extracts (Ethylacetate root extract (ERE), Butanol root extract (BRE), Ethylacetate leaf extract (ELE) and Butanol leaf extract (BLE) of *C. procera*) were substituted with $CaCl_2$, the inductive effects of the extracts were observed.

Determination of Atpase Activity

The Lardy and Wellman (1953) method was modified to access the mitochondrial ATPase activity. 65 mM Tris-HCL (pH 7.4), 0.5 mg mitochondrial protein, 0.5 mM KCl, 1 mM ATP, and 25 mM sucrose were all present in each test medium. The extracts (ERE, BRE, ELE, and BLE extracts) were introduced with varying quantities as needed. The ATP was added to start the reaction, which was then allowed to run for 30 minutes at 37°C with constant shaking. Each test tube's mixture received 1 ml of 10% sodium dodecyl sulfate to bring the reaction to a halt. Each test tube was then filled with 4 ml of distilled water before having 1ml of the resulting solution transferred into brand-new test tubes and one milliliter of 1.25% Ammonium Molybdate in 6.5% Sulphuric Acid added. 1 ml of 9% ascorbic acid was added for the expected 660 nm color development. The entire analysis was performed in triplicate.

Determination of Mitochondria MDA Level

Thiobarbituric acid reactive substances (TBARS), and malondialdehyde (MDA) was quantified by the method described by Aeschbach *et al.*, 1994

$$\textbf{MDA}\ (\text{units/mg of protein}) = \frac{Absorbance \times volume\ of\ mixture}{E532 \times volume\ of\ sample \times mg\ of\ protein}$$

Where, E532 = 1.56×10^{-5}

Molecular Docking and Molecular Simulation

Protein and ligands three-dimensional structures were produced in pdb format. Autodock vina conducted the molecular docking simulation. Autodock vina is a program for virtual screening that can be used in computational drug discovery to check libraries of compounds against possible therapeutic targets. Pharmaceutical Chemists can execute Virtual Screening using Autodock vina from any platform, and the software supports users at every stage of the procedure, from data preparation through job submission and outcome analysis. The AutodockTools (ADL) was used to reduce energy and add the partial charges of the receptor's polar hydrogens (protein). The protein was created in a static (stiff) shape, whereas the ligands were created with flexible torsion angles. Additionally, proteins and their ligands were stored in pdbqt forms that are appropriate for docking simulation. Total intermolecular energies (kcal/mol), including electrostatic, hydrogen bond, and Van Der Walls force energies, were used to compute the affinity binding. On the other hand, internal ligand energy is also stimulated to cause the proper torsion angles of the ligand. In order to choose the optimum binding mode, the docking algorithm analyzed the lowest binding energy (LBE).

Molecular Simulation

For the MD simulation, the GROMACS (Version 2018) was used (Abraham *et al.*, 2015). All complexes were subjected to MD simulation using the single-point charge (SPC) water model and the GROMOS54a7 force field. PRODRG server was used to create the topologies and parameter files for the lead compounds and the standard inhibitor (Schüttelkopf and Van Aalten, 2004). Simulated complexes were all contained in a cube with a 1- buffer distance. The appropriate quantity of ions were added to the complexes to electro-neutralize them. By applying 5,000 steps of the steepest descent method, bad connections and collisions in the protein were eliminated. All of the complexes went through two steps of equilibration after the energy minimization, the first being 100 ps of NVT equilibration and the second being 100 ps of NVT equilibration. Temperature coupling was used to overcome the problem of the cold solute-hot solvent by indexing the system into non-water and water components using the GROMACS gmx make ndx module (Lemkul, 2019). A Berendsen thermostat was used to keep the system's temperature at 300°C (Berendsen *et al.*, 1995). Similarly, a Parrinello-Rahman barostat was used to maintain the system's pressure (Parrinello and Rahman, 1981). The LINCS approach was used to address the system's long-range interaction (Hess *et al.*, 1997). MD simulations were run for 50,000 ps, and the coordinates for the entire system were stored every 1 ps. The GROMACS package's numerous analysis modules were used to undertake structural and conformational analysis on all systems.

Statistical Analysis

Student's T-test and one-way analysis of variance (ANOVA) were used to statistically examine the data. Every outcome was shown as Mean Standard Deviation (SD). P values lower than 0.05($P<0.05$) were regarded as statistically significant.

Results and Discussion

Mitochondrial Swelling, Atpase activity and Lipid peroxidation

Effects of the butanol leaves extract (BLE), ethylacetate leaves extract (ELE), butanol root extract (BRE), and ethylacetate root extract (ERE) of the *C. procera* plant on the MMPT pore at various dosages (40, 50, and 60 mg/100g bw) were assessed.

In the absence of calcium, there were no significant changes in the volume of intact respiring mitochondria powered on succinate, but calcium ion produced considerable opening of the MMPT pore (Fig. 1). The typical pore inhibitor, spermine, reversed the observed induction.

At all tested dosages, the BLE of *C. procera* caused the opening of the mitochondrial membrane permeability transition pore in intact mitochondria (Fig. 2) with 6.6, 7.4, and 5.9-fold increases seen in the groups treated with 40, 50, and 60 mg/100g bw, respectively. Spermine reversed every opening that was observed. Furthermore, in intact mitochondria treated with the ELE of *C. procera* at the dosages used, swelling of the mitochondrial membrane was seen (Fig. 3). Fold increases of 10.2, 7.3, and 6.4 were noted in the groups given 40, 50, and 60 mg/100g bw, respectively with spermine reversal. At all tested dosages, *C. procera* BRE caused the opening of the MMPT pore (Fig. 4); 12.21, 10.12, and 20.40 folds increase were seen in the groups treated with 40, 50, and 60 mg/100g bw, respectively. Spermine reversed each and every openings that was observed. ERE of *C. procera* treatment of intact mitochondria resulted in 11.37, 11.84, and 5.52 fold increases in MMPT pore opening, in the groups treated with 40, 50, and 60 mg/100g bw, respectively (Fig. 5). Spermine reversed every opening that had been seen.

At all studied concentrations (Fig. 6), the BLE, ELE, BRE, and ERE of *C. procera* considerably increased the activity of mitochondrial ATPase, indicating that the components of the plant enhanced ATP hydrolysis.

In order to ascertain the effects of the plant extracts on the production of free radicals, the mitochondrial levels of malondialdehyde (MDA) in rat livers treated with the extracts of *C. procera* were quantified. The findings demonstrated that all tested doses of the extracts significantly ($P<0.05$) increased the levels of mitochondrial MDA in comparison to the untreated group except for the 50mg/100g bw dose of ethylacetate leaf extract which has no significant reduction when compared to the untreated rats (Fig. 7).

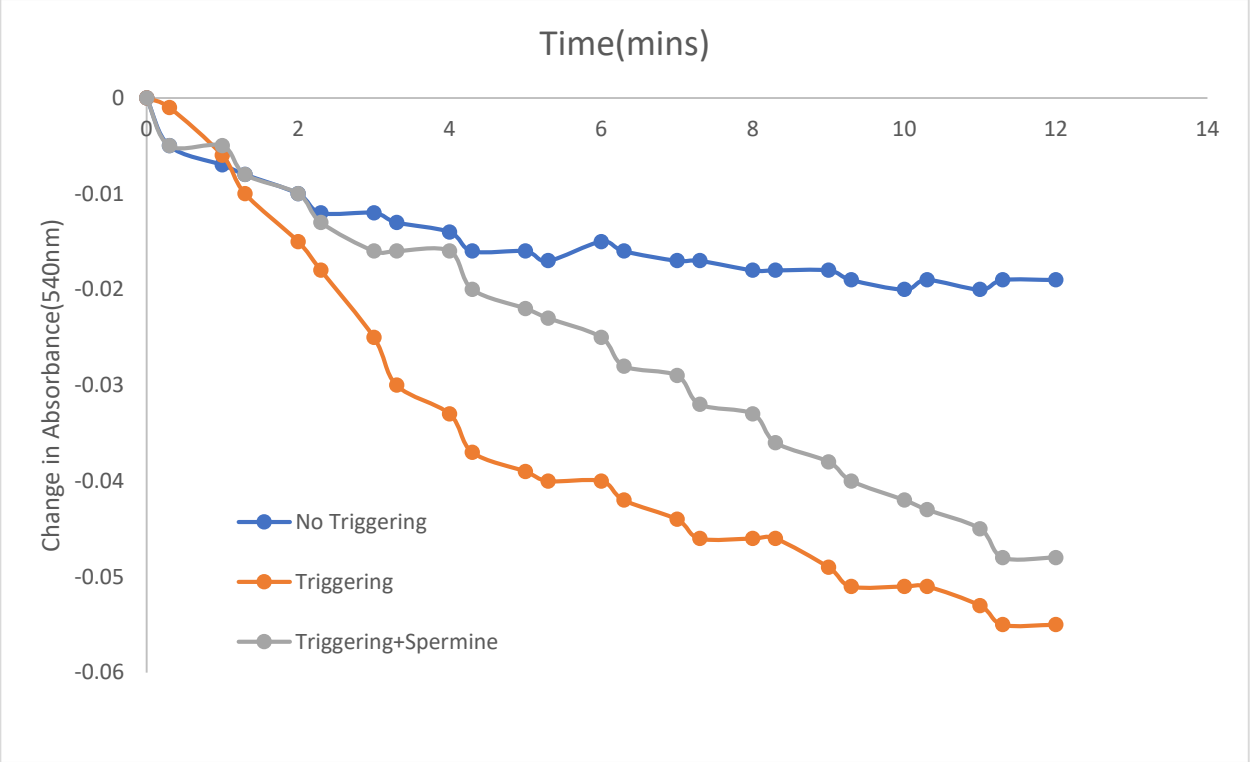

Figure 1: *In vivo* induction of the opening of MMPT pore by Ca^{2+} and reversal by spermine

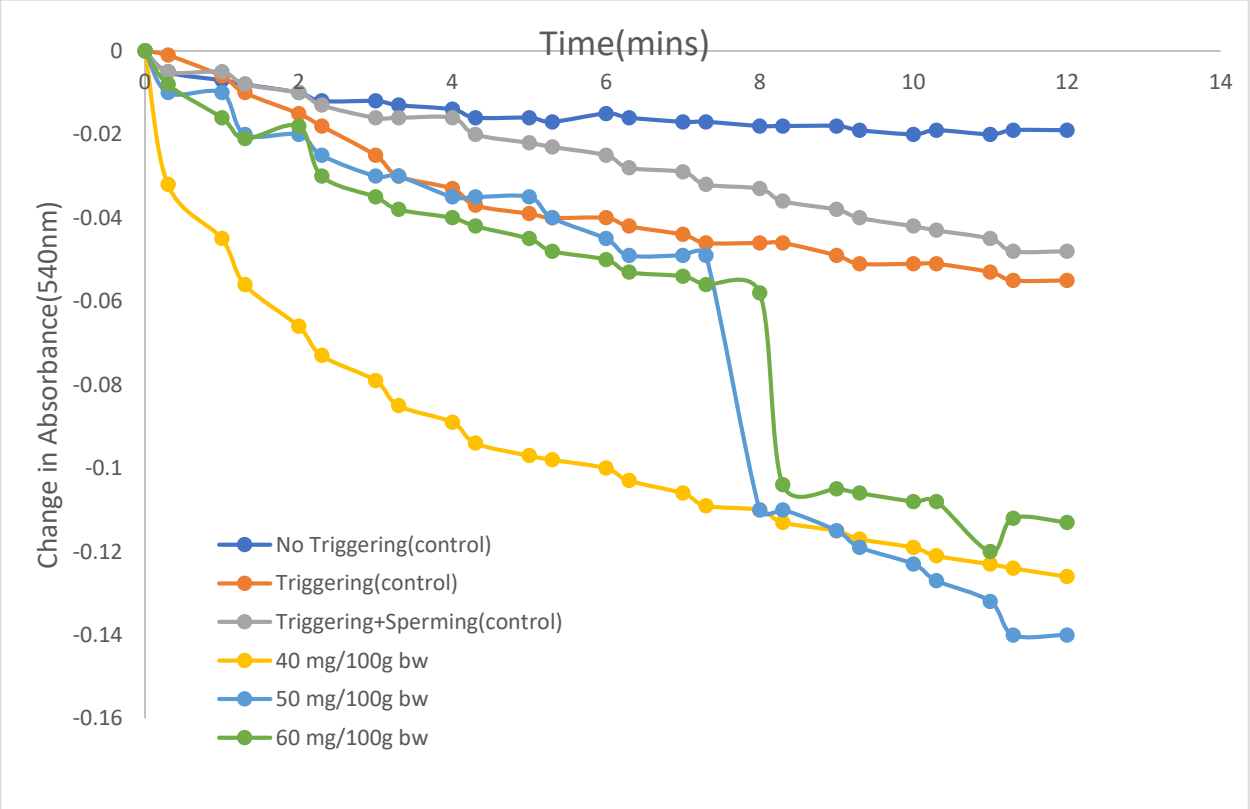

Figure 2: The effect of butanol leaf extract of *Calotropis procera* on MMPT pore at varying concentration**.**

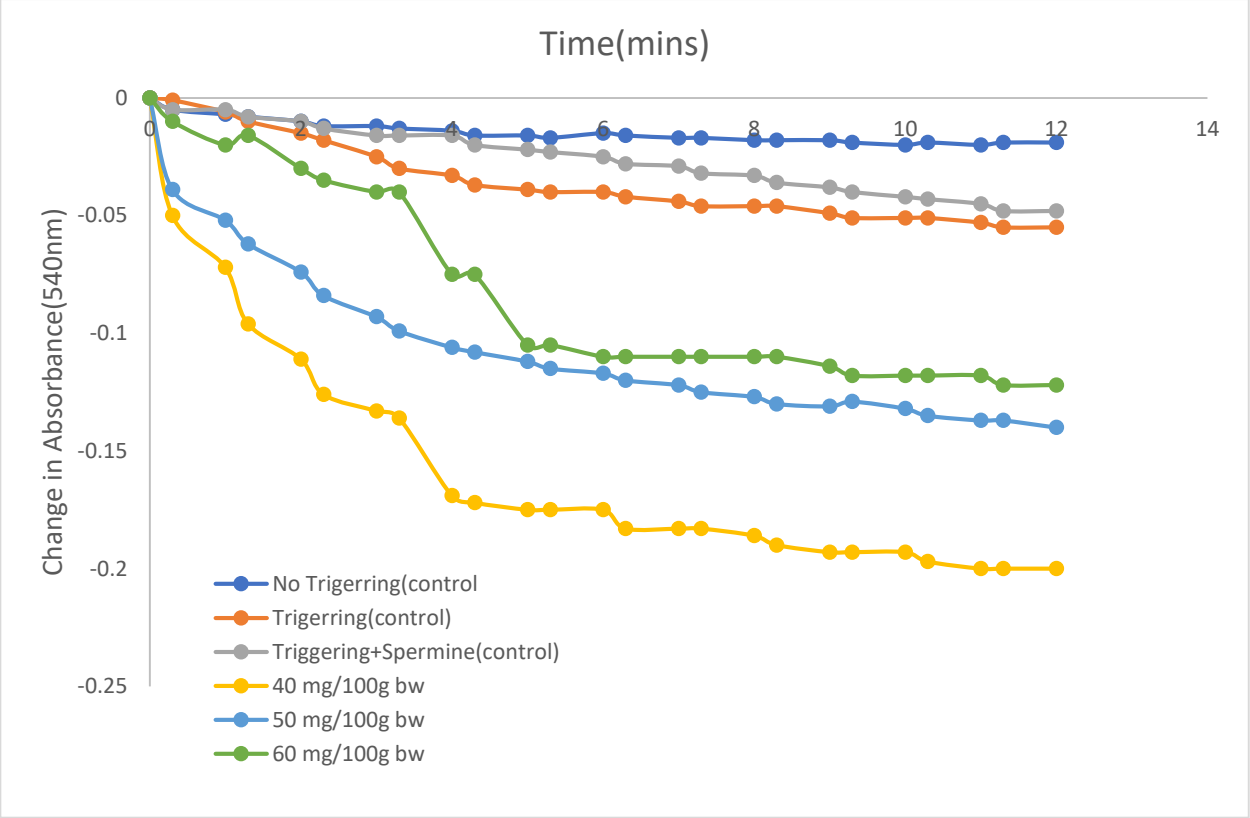

Figure 3: The effect of ethylacetate leaf extract of *Calotropis procera* on MMPT pore at varying concentration**.**

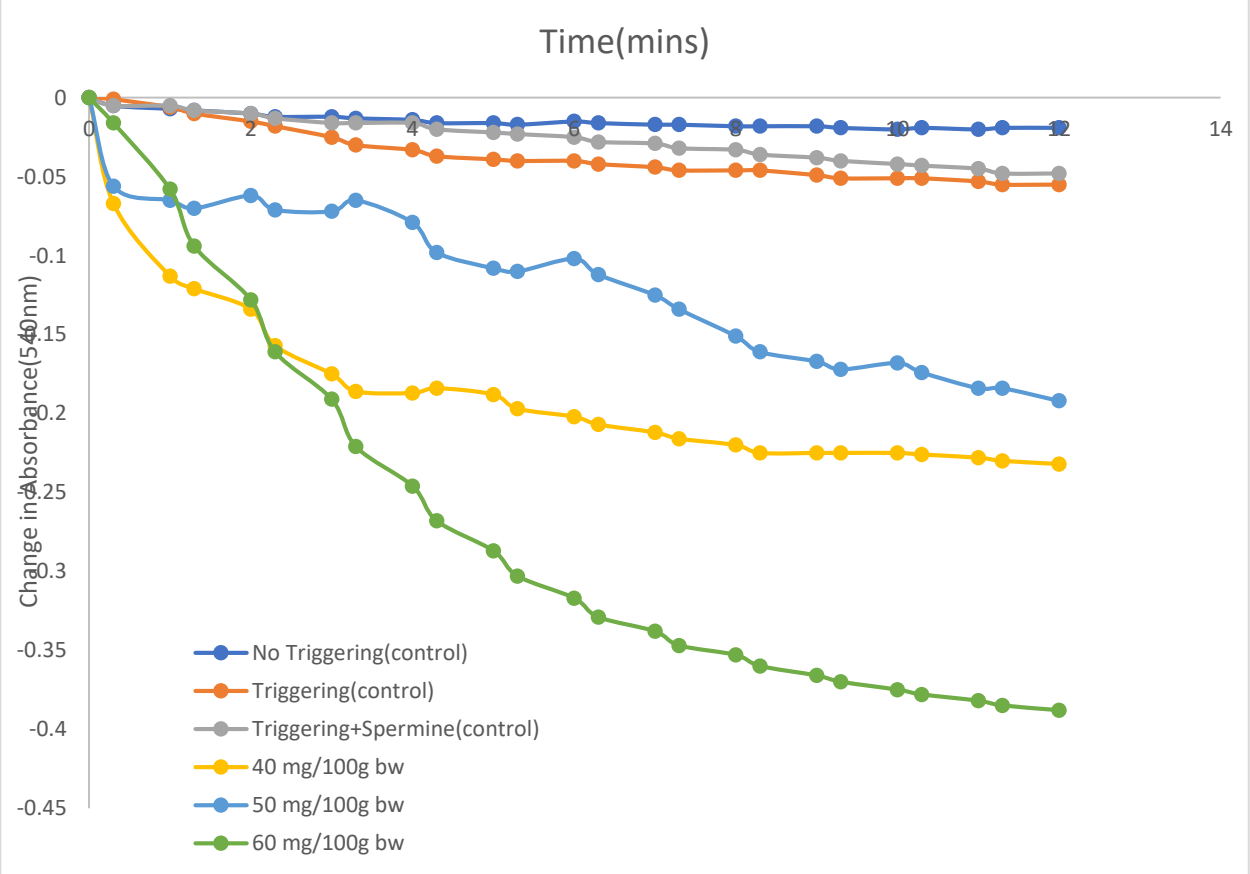

Figure 4: The effect of butanol root extract of *Calotropis procera* on MMPT pore at varying concentration**.**

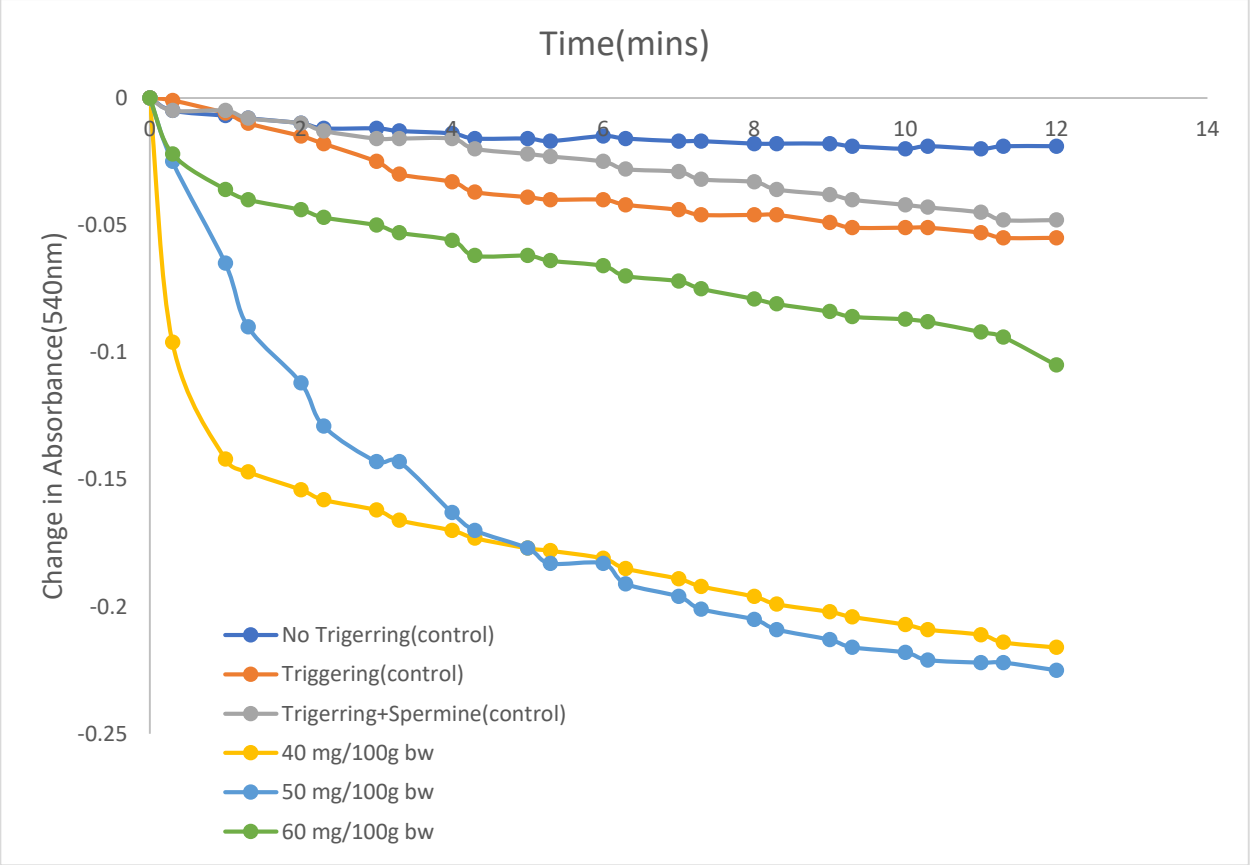

Figure 5: The effect of ethylacetate root extract of *Calotropis procera* on MMPT pore at varying concentration**.**

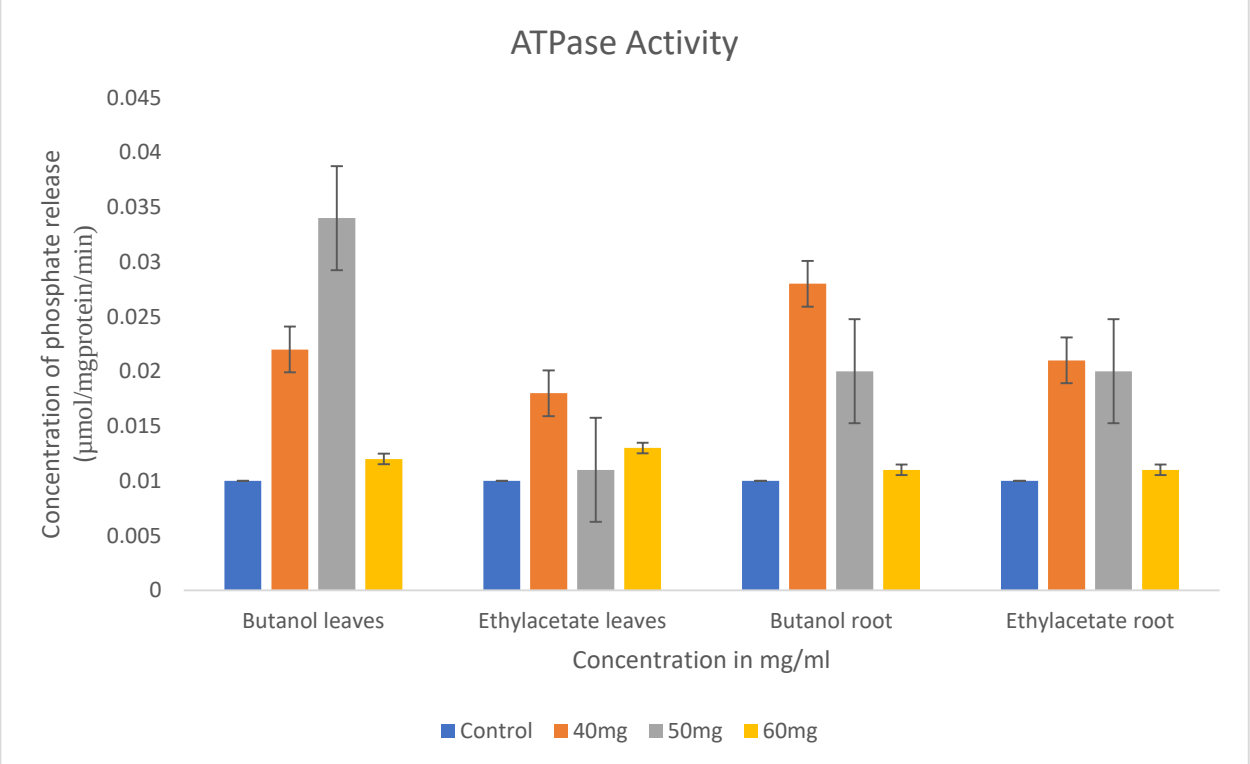

Figure 6: The effects of varying doses of extracts of *Calotropis procera* on mitochondria ATPase activities.

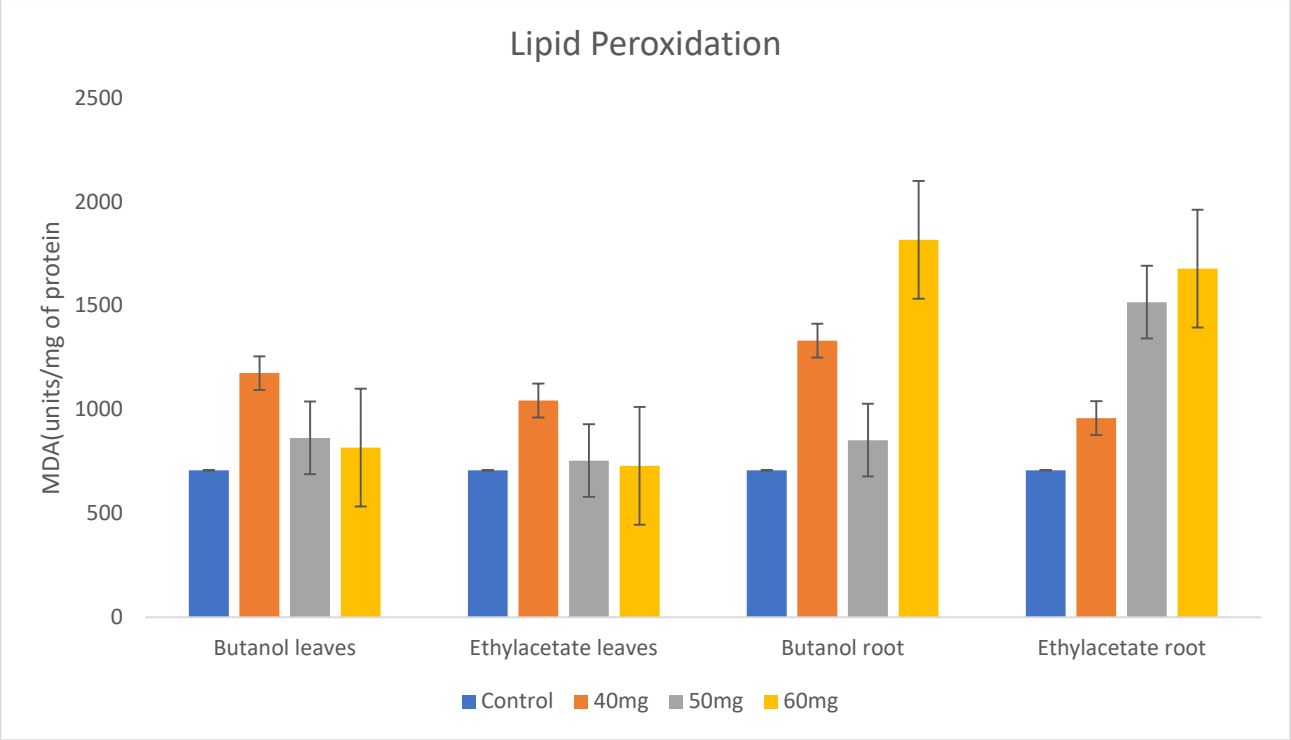

Figure 7: MDA levels in the liver mitochondria of male Wistar rats intubated with varying doses of root ethylacetate, root butanol, leaves ethylacetate and leaves butanol extracts of *Calotropis procera*

Pharmacotherapy is beginning to focus on the mitochondrial permeability transition pore (MMPTP), an unending pore in the inner membrane of the mitochondria (Bhosale and Duchen, 2019). The activation of the apoptotic cascade and subsequent step-by-step cell death are caused by the opening of this pore (Javadov *et al.*, 2009). It implies that highly proliferating cells in conditions like cancer may be killed by this pore openings. Another therapeutic angle is to stop the pore from developing (Martel *et al.*, 2012). The opening of the mitochondrial membrane permeability transition pore is a crucial apoptotic stage because it signals the cell's ultimate decision to commit suicide by releasing cytochrome C into the cytosol (Newmeyer *et al.*, 1994). The mitochondria are the powerhouse and arsenal of the cells' suicide weapons. The permeabilization of the mitochondrial outer membrane, which results from the convergence of numerous deadly signal transduction pathways, triggers the release of pro-apoptotic proteins from the cytosol, which interferes with the bioenergetic components of mitochondria (Ehigie *et al.*, 2019). In traditional medicine, the genus Calotropis is used to treat leprosy, ulcers, tumors, spleen and liver problems, and piles. It also works as a purgative, antihelmintic, anticoagulant, antipyretic, analgesic, antiinflammatory, and antibacterial, as well as a palliative for breathing and blood pressure disorders. It also acts as a neuromuscular blocker (Jalalpure *et al.*, 2009; Mukherjee *et al.*, 2009; Patra *et al.*, 2009; Seddek *et al.*, 2009). Members of the family are high in cardiac glycosides and are thought to be potential anticancer agents (Barrett & Kieffer, 2001). This study was carried out to investigate if *C. procera* will induce apoptotic effect in healthy male wistar rats. The inductive effects of all extracts were assayed using mitochondria swelling assay as a predictive measurement. Opening of the pore was observed at all the tested dosages (40 mg/100 g, 50 mg/100 g and 60 mg/100 g) of the plant extracts, suggesting that *Calotropis procera* leaves and root contain bioactive ingredients with potential to open the MMPT pore and commits cells to apoptosis. Interestingly, various fold increases were observed at different concentration of the extracts which are 6.63,7.4 and 5.90 for LBE and 10.2,7.37 and 6.4 for LEE at all doses 40 mg/100 g BW, 50 mg/100 g BW and 60 mg/100 g BW respectively, with a much higher inductive effect being observed at some concentrations from the root extracts whch are 12.21,10.1 and 20.4 for RBE and 11.37,11.84,5.52 for REE at different doses of 40 mg/100 g BW, 50 mg/100 g BW and 60 mg/100 g BW respectively. These observed large amplitude swellings caused by the plant extracts suggest a possible role for the medicinal plant in the treatment of ailments arising from apoptosis deregulation such as cancer.

Also, ATP hydrolysis was enhanced by the extracts of *C. procera* (Fig. 6). This was quantified by the release of inorganic phosphate. ATP synthase, an enzyme responsible for the synthesis of ATP in an intact mitochondrion is also responsible for its hydrolysis when the electrochemical gradient of the inner mitochondrial membrane is breaded (Neginskaya *et al.*, 2015). Inorganic phosphate release an indication of the uncoupling of phosphorylation in the mitochondrion, a process which is synonymous with MMPT pore opening and mitochondrial swelling. The results from fig. 7 shows that there is significant ($p< 0.05$) increase in the level of mitochondria MDA (Malonyldialdehyde) level in treated groups when compared to the control, Mitochondria swelling leads to the disruption of calcium level and increase in the production/accumulation of reactive oxygen species(ROS) (Akhter *et al, 2017).*

Moleculare docking study

In docking, it is essential to comprehend how a protein receptor locates and binds its ligand. Protein-ligand interactions facilitate substrate ranking and prediction (Sousa *et al.*, 2006). Emodin is a proven compound that has been said to be involved in human cyclophilin D expression both in the wet laboratory and in molecular studies (Zhang *et al.*, 2017) was used as a standard for the plant phytochemicals in the *In-silico* studies.

Molecular docking of 2"- Oxovoruscharin and Emodin in complex with Cyclophylin D (CypD)

Table 1: Protein–ligand interaction profiles. The table reveals the various interactions and binding affinities of phytochemicals in *Calotropis procera*.

Ligands	**Number of hydrogen bonds**	**Binding affinity** Kcal/Mol
2"-Oxovoruscharin	2	-7.9
Calactin	1	-7.7
Taraxasterol acetate	none	-7.7
3-O-beta-Allopyranosyl-(1->4)-beta-oleandropyranosyl-11-O-isobutyryl-12-O-acetyltenacigenin B	2	-7.6
Taraxasterol	none	-7.5
Rutin	4	-7.3
Benzoyllineolone	3	-7.3
Lupeol acetate	2	-7.2
Narcissoside	1	-7.1
Quercetin	3	-7.0
Quercetin 3,3'-dimethyl ether	3	-6.7
Azaleatin	2	-6.7
Isoquercitrin	2	-6.5
3-Hydroxy-3',4',5,7-tetramethoxyflavone	1	-6.4
14beta-Pregn-5-en-20-one	1	-6.3
14beta,17alpha-Pregn-5-en-20-one, 3beta,8,12beta,14-tetrahydroxy-	1	-6.3
Isorhamnetin	3	-6.3
2-aminoethyl beta-D-glucopyranosyl-(1->3)-beta-D-glucopyranosyl-(1->3)-beta-D-glucopyranosyl-(1->3)-beta-D-glucopyranosyl-(1->3)-{6-O-[beta-D-glucopyranosyl-(1->3)-beta-D-glucopyranosyl]-beta-D-glucopyranosyl}-beta-D-glucopyranosyl-(1->3)-beta-D-glucopyranosyl-(1->3)-beta-D-glucopyranosyl-(1->3)-beta-D-glucopyranoside	none	-5.8
alpha-Amyrinacetate	none	-5.7
Methyl caffeate	4	-5.6
D-Glucose	7	-4.7

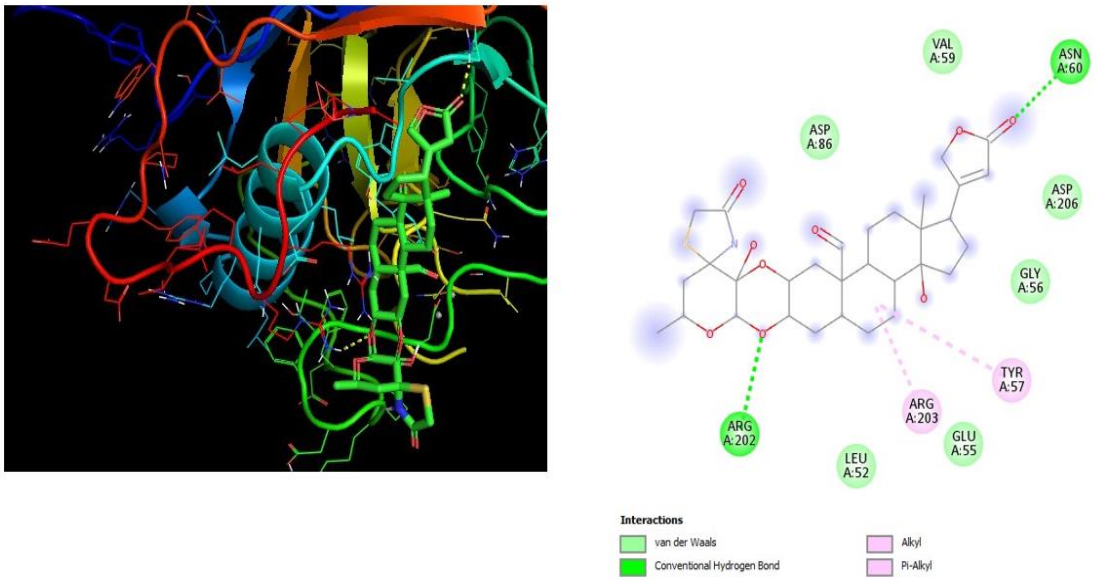

Figure 8: 3D and 2D representation of 2″- Oxovoruscharin in complex with Cyclophylin D (CypD)

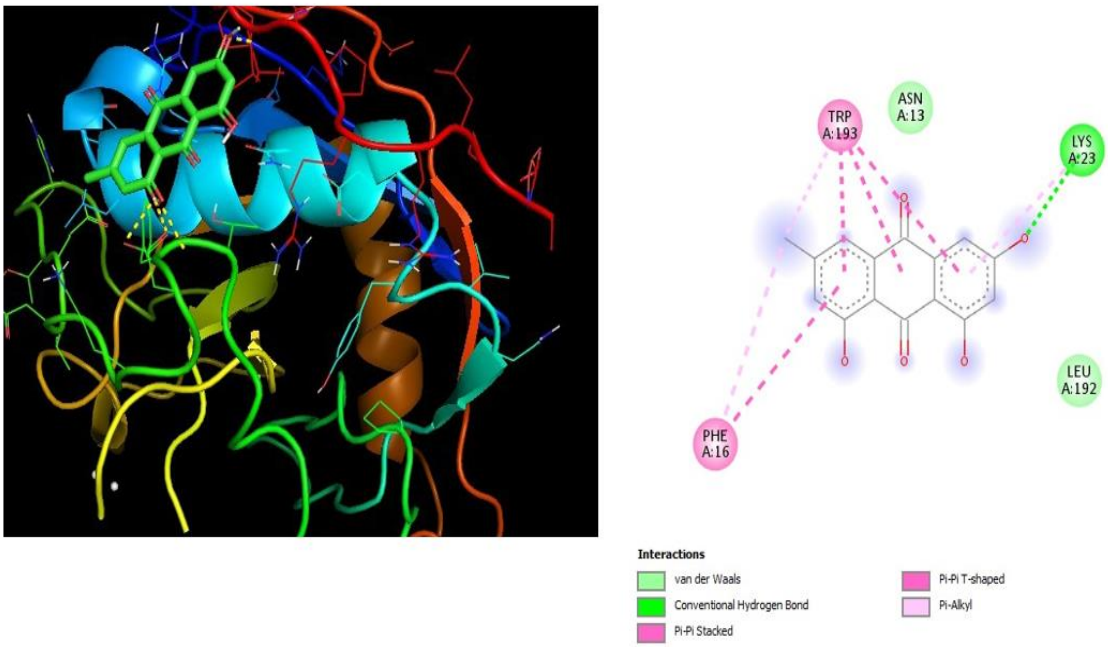

Figure 9: 3D and 2D representation of Emodin in complex with Cyclophylin D (CypD)

Molecular Simulation study

On the basis of the docking study, 2"-Oxovoruscharin was selected for a molecular dynamics simulation of the system to examine the dynamics behavior of the target protein. This ligand exhibits the greatest binding contact and hydrogen conformational binding. Using the following indices, the stability of the pre- and post-simulation protein-ligand combinations may be evaluated based on the trajectory provided by the molecular dynamic simulation. Hydrogen-bonding interaction, solvent-accessible surface area, mean-square deviation and variance. The molecular dynamic simulation trajectory reveals the stability of the protein-ligand configurations in prior to and after simulation and can be measured using the following indices: Radius of gyration, root mean square deviation, root mean square fluctuation, solvent accessible surface area, and hydrogen bond interaction. Radius of gyration indicate that at the beginning, the atoms of Cyclophilin D-Oxovoruscharin (CycD-lig) complex loses their compactness and become less stable at time intervals of 0 picoseconds(ps) to 5000 ps. The radius of gyration indicates that the atom exhibits strong stability from 10000ps and reveals that a compactness occurs till at time intervals of 50000 ps. Finally, when compared with the Cyclophilin D-Emodin (CycD-emodin) complex, 2”- Oxovoruscharin gyrate more (i.e it’s less stable compared with emodin a proven standard).

The Root Mean Squared deviation (RMSD) figure shown in Figure 10(B) demonstrates that the complex apo_ligand (i.e Cyclophilin D-Oxovoruscharin) RMSD fluctuates at 0.3 (nm), with a little variation near 0.35 (nm), and the fluctuation peaks lower near the simulation's conclusion. This demonstrates that the structure is less stable, as the stability increases and the structural deviation decreases with decreasing RMSD. Apo_emodin complex shows less deviation (i.e less conformational changes from the original Cyclophilin D). Root Mean Squared fluctuations (RSMF) greater than 0.25 nm are of interest. For instance, the fluctuation near the atom at position near 50, the position near 75, position 150 and the position near 200. They are the main atoms that make up the protein's general structure according to the RMSD; there is also not a lot of variation because it happens between 0.1 and 0.2. With the aid of molecular visualization tools like VMD, the specific atoms in the complex—that is, the specific atom out of the complex that participates in the fluctuation—are examined. The forcefield's constraints and the simulation's atoms' movement and vibration around an equilibrium structure are both contributing factors to the disparity, although CycD-emodin shows less residue fluctuation.

Figure 11(D) shows an illustration of the Solvent Accessible Surface (SASA). The graph demonstrates how the atoms are rigidly packed and more stable near a surface area solvent. CycD-lig complex shows a high surface area at the start than that of the Emodin complex. We need lesser area to be exposed to water because solvent interaction can affect the conformational/stability of protein.

The hydrogen-bonding of the protein to the 2″-Oxovoruscharin (lig.) and Emodin is depicted in Fig. 11(E). A balance of lipophilic and hydrogen bonding groups is necessary for the ligand to have the best binding potency and selectivity. The five rules of Lipinski (Ro5) helped medicinal chemists achieve a better balance of attributes inside a therapeutic molecule (Alex *et al.*, 2011). The logical conclusion is that not breaking more than one of these rules should result in a lower attribution of pharmacokinetics in the early stages of development.

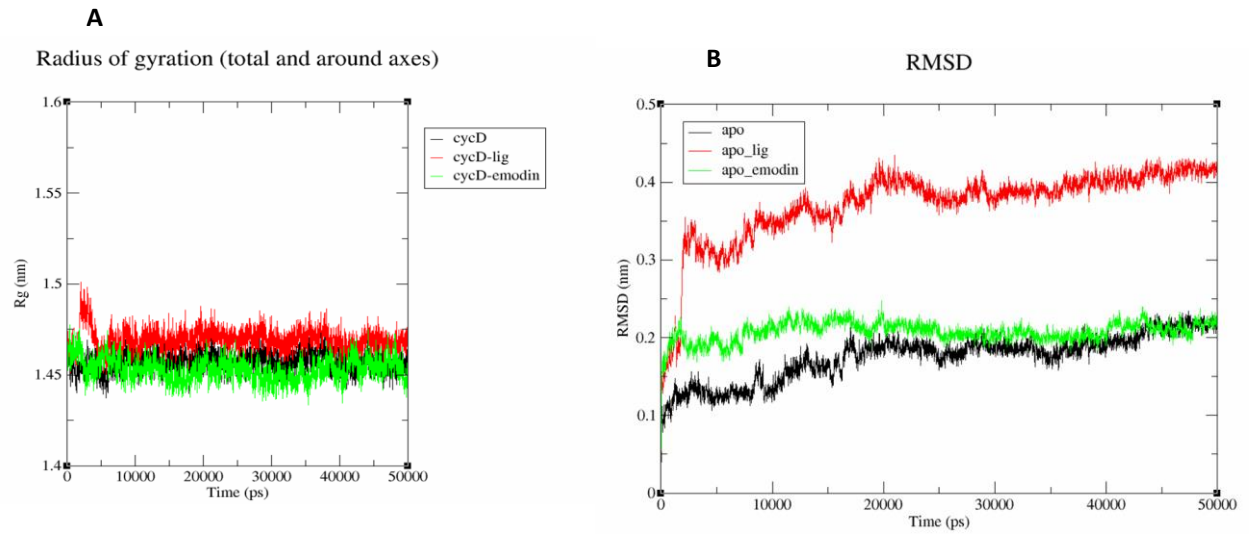

Figure 10: (**A)** Gyrate plot of the molecular dynamics simulation using GROMACS. A plot of Radius of Gyration (Rg) in nanometres (nm) against time in picoseconds (ps). The Gyration was observed 50000ps and (**B**) Root mean square deviation (RSMD) plot of the molecular dynamics simulation using GROMACS. A plot of RSMD in nanometres (nm) against time in picoseconds (ps).

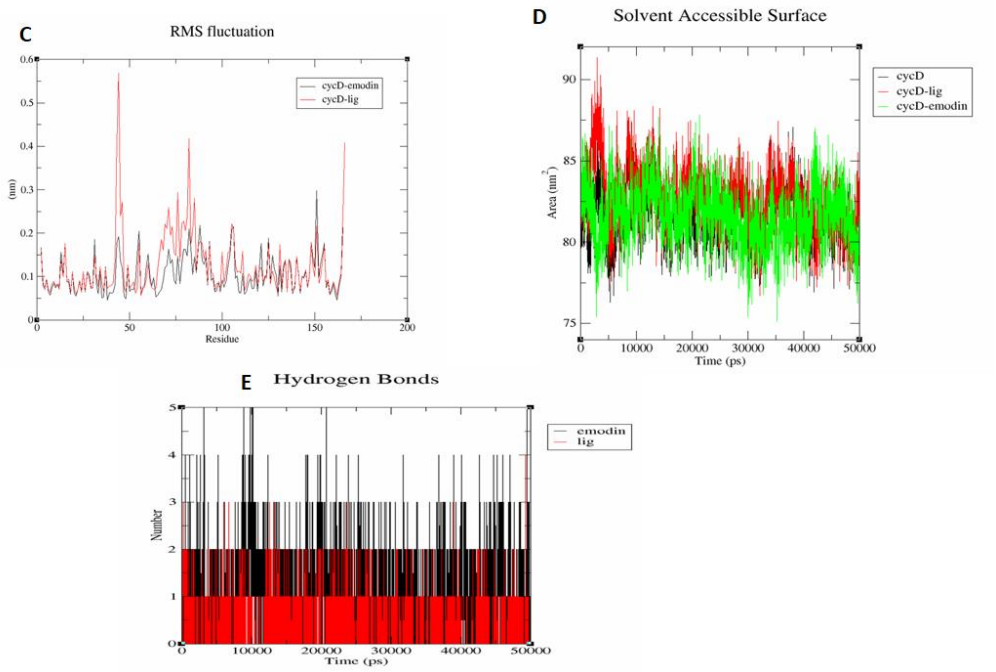

Figure 11: **(C)** Root mean square fluctuation (RSMF) plot of the molecular dynamics simulation using GROMACS. A plot of RSMF in nanometres(nm) against Atom/Residue in grams(g) and **(D)** Solvent Accessible Surface(SASA) plot of the molecular dynamics simulation using GROMACS. A plot of RSMD in nanometres(nm^2) against time in picoseconds(ps) and **(E)** The average number of intermolecular H-bonds of 2″- Oxovoruscharin (lig.) and Emodin in complex with Cyclophylin D (CypD).

Conclusion

Conclusively, this study portrayed that the plant extracts of *C. procera* show profound MMPTP induction and enhanced ATPase hydrolysis. This *in vivo* data suggests that the plant extracts of *C. procera* has pro-apoptotic activity and thus be considered for further studies. The observed inducing effect could be responsible for its therapeutic potential towards disease arising from cell proliferation through intrinsic apoptotic pathway. However, fractionation of the extracts is recommended to identify the bioactive phytocompound(s) responsible for the observed inducing effects. In addition to revealing the molecular interaction between the components, analysis of the docked complexes shows the molecular interaction between the components. The binding pattern of amino acid residues influences the interaction energy of docked complexes. Using Lippinski's rule, docking with Cyclophilin D, which has exceptionally negative binding energy values, demonstrated the therapeutic activity of the

bioactive compounds identified from *C. procera*. The interaction of 2"-Oxovoruscharin, which has a binding energy of -7.9 kcal/mol, with the receptor indicates that a compound with a bigger negative binding energy value may form a stable complex. The findings from the wet laboratory were backed by the results of the dynamic modeling, which demonstrated that the phytochemical interact with the protein in a rather stable conformation with a higher binding energy.

Conflict of Interest: No conflict of interest

References

Abraham, M. J., Murtola, T., Schulz, R., Páll, S., Smith, J. C., Hess, B., & Lindahl, E. (2015a). GROMACS: High performance molecular simulations through multi-level parallelism from laptops to supercomputers. *SoftwareX*, *1*, 19–25.

Abraham, M. J., Murtola, T., Schulz, R., Páll, S., Smith, J. C., Hess, B., & Lindahl, E. (2015b). GROMACS: High performance molecular simulations through multi-level parallelism from laptops to supercomputers. *SoftwareX*, *1*, 19–25.

Aeschbach, R., Löliger, J., Scott, B., Murcia, A., Butler, J., Halliwell, B., & Aruoma, O. (1994). Antioxidant actions of thymol, carvacrol, 6-gingerol, zingerone and hydroxytyrosol. *Food and Chemical Toxicology*, *32*(1), 31–36.

Agarwal, A., Wu, P.-H., Hughes, E. G., Fukaya, M., Tischfield, M. A., Langseth, A. J., Wirtz, D., & Bergles, D. E. (2017). Transient opening of the mitochondrial permeability transition pore induces microdomain calcium transients in astrocyte processes. *Neuron*, *93*(3), 587–605.

Agbaje, E., & Adeniran, J. (2009). Some Gastrointestinal Effects of the Aqueous Root Extract of Plumbago Zeylanica (Lead Wort). *African Journal of Biomedical Research*, *12*(1), 63–68.

Ajayi, E. I. O., Modo, E. U., Adebamowo, A. O., Banerjee, U. C., Tewe, O. O., & Olorunsogo, O. O. (2016). Inhibitory activity of ethanol extract of Manihot esculenta on mitochondrial membrane permeability transition pore and caspase 3 in type 2 diabetes mellitus. *Int J Biochem Res Rev*, *9*(4), 1–10.

Akhter, F., Chen, D., Yan, S. F., & Yan, S. (2017). Mitochondrial perturbation in Alzheimer's disease and diabetes. *Progress in Molecular Biology and Translational Science*, *146*, 341–361.

Al Sulaibi, M. A., Thiemann, C., & Thiemann, T. (2020). Chemical constituents and uses of Calotropis procera and Calotropis gigantea–a review (Part I–the plants as material and energy resources). *Open Chemistry Journal*, *7*(1).

Azarpajouh, S., Calderón Díaz, J., Bueso Quan, S., & Taheri, H. (2021). Farm 4.0: Innovative smart dairy technologies and their applications as tools for welfare assessment in dairy cattle. *CABI Reviews*, *2021*.

Barrett, B., & Kieffer, D. (2001a). Medicinal plants, science, and health care. *Journal of Herbs, Spices & Medicinal Plants*, *8*(2–3), 1–36.

Barrett, B., & Kieffer, D. (2001b). Medicinal plants, science, and health care. *Journal of Herbs, Spices & Medicinal Plants*, *8*(2–3), 1–36.

Batool, H., Hussain, M., Hameed, M., & Ahmad, R. (2020). A review on Calotropis procera its phytochemistry and traditional uses. *Big Data Agric*, *2*, 29–31.

Bauer, T. M., & Murphy, E. (2020). Role of mitochondrial calcium and the permeability transition pore in regulating cell death. *Circulation Research*, *126*(2), 280–293.

Berendsen, H. J., van der Spoel, D., & van Drunen, R. (1995). GROMACS: A message-passing parallel molecular dynamics implementation. *Computer Physics Communications*, *91*(1–3), 43–56.

Bernardi, P., Broekemeier, K. M., & Pfeiffer, D. R. (1994). Recent progress on regulation of the mitochondrial permeability transition pore; a cyclosporin-sensitive pore in the inner mitochondrial membrane. *Journal of Bioenergetics and Biomembranes*, *26*, 509–517.

Bernardi, P., & von Stockum, S. (2012). The permeability transition pore as a Ca2+ release channel: New answers to an old question. *Cell Calcium*, *52*(1), 22–27.

Beutner, G., Alanzalon, R. E., & Porter Jr, G. A. (2017). Cyclophilin D regulates the dynamic assembly of mitochondrial ATP synthase into synthasomes. *Scientific Reports*, *7*(1), 14488.

Bhosale, G., & Duchen, M. R. (2019). Investigating the mitochondrial permeability transition pore in disease phenotypes and drug screening. *Current Protocols in Pharmacology*, *85*(1), e59.

Bibli, S.-I., Papapetropoulos, A., Iliodromitis, E. K., Daiber, A., Randriamboavonjy, V., Steven, S., Brouckaert, P., Chatzianastasiou, A., Kypreos, K. E., & Hausenloy, D. J. (2019). Nitroglycerine limits infarct size through S-nitrosation of cyclophilin D: a novel mechanism for an old drug. *Cardiovascular Research*, *115*(3), 625–636.

Bonora, M., Morganti, C., Morciano, G., Pedriali, G., Lebiedzinska-Arciszewska, M., Aquila, G., Giorgi, C., Rizzo, P., Campo, G., & Ferrari, R. (2017). Mitochondrial permeability transition involves dissociation of F1 FO ATP synthase dimers and C-ring conformation. *EMBO Reports*, *18*(7), 1077–1089.

Bonora, M., Wieckowski, M. R., Chinopoulos, C., Kepp, O., Kroemer, G., Galluzzi, L., & Pinton, P. (2015). Molecular mechanisms of cell death: Central implication of ATP synthase in mitochondrial permeability transition. *Oncogene*, *34*(12), 1475–1486.

Danial, N. N., & Korsmeyer, S. J. (2004). Cell death: Critical control points. *Cell*, *116*(2), 205–219.

Dhileepan, K. (2014). Prospects for the classical biological control of Calotropis procera (Apocynaceae) using coevolved insects. *Biocontrol Science and Technology*, *24*(9), 977–998.

Ehigie, L. (2019). Inductive effects of fractions of crude water-soluble extract of Momordica charantia on rat liver mitochondrial membrane permeability transition pore. *African Journal of Medicine and Medical Sciences*, *48*(3), 319–327.

Elrod, J. W., Wong, R., Mishra, S., Vagnozzi, R. J., Sakthievel, B., Goonasekera, S. A., Karch, J., Gabel, S., Farber, J., & Force, T. (2010). Cyclophilin D controls mitochondrial pore–dependent Ca 2+ exchange, metabolic flexibility, and propensity for heart failure in mice. *The Journal of Clinical Investigation*, *120*(10), 3680–3687.

Giorgio, V., Fogolari, F., Lippe, G., & Bernardi, P. (2019). OSCP subunit of mitochondrial ATP synthase: Role in regulation of enzyme function and of its transition to a pore. *British Journal of Pharmacology*, *176*(22), 4247–4257.

Glancy, B., & Balaban, R. S. (2012). Role of mitochondrial Ca2+ in the regulation of cellular energetics. *Biochemistry*, *51*(14), 2959–2973.

Hassan, L. M., Galal, T. M., Farahat, E. A., & El-Midany, M. M. (2015). The biology of Calotropis procera (Aiton) WT. *Trees*, *29*, 311–320.

Hess, B., Bekker, H., Berendsen, H. J., & Fraaije, J. G. (1997). LINCS: A linear constraint solver for molecular simulations. *Journal of Computational Chemistry*, *18*(12), 1463–1472.

Jalalpure, S., Salahuddin, M., Imtiyaz Shaikh, M., & Manvi, F. (2009). Anticonvulsant effects of Calotropis procera root in rats. *Pharmaceutical Biology*, *47*(2), 162–167.

Javadov, S., & Kuznetsov, A. (2013). Mitochondrial permeability transition and cell death: The role of cyclophilin d. *Frontiers in Physiology*, *4*, 76.

Karch, J., Bround, M. J., Khalil, H., Sargent, M. A., Latchman, N., Terada, N., Peixoto, P. M., & Molkentin, J. D. (2019). Inhibition of mitochondrial permeability transition by deletion of the ANT family and CypD. *Science Advances*, *5*(8), eaaw4597.

Kokoszka, J. E., Waymire, K. G., Levy, S. E., Sligh, J. E., Cai, J., Jones, D. P., MacGregor, G. R., & Wallace, D. C. (2004). The ADP/ATP translocator is not essential for the mitochondrial permeability transition pore. *Nature*, *427*(6973), 461–465.

Kroemer, G., Dallaporta, B., & Resche-Rigon, M. (1998). The mitochondrial death/life regulator in apoptosis and necrosis. *Annual Review of Physiology*, *60*(1), 619–642.

Lapidus, R. G., & Sokolove, P. M. (1993). Spermine inhibition of the permeability transition of isolated rat liver mitochondria: An investigation of mechanism. *Archives of Biochemistry and Biophysics*, *306*(1), 246–253.

Lehmkuhl, O., Houzeaux, G., Owen, H., Chrysokentis, G., & Rodríguez, I. (2019). A low-dissipation finite element scheme for scale resolving simulations of turbulent flows. *Journal of Computational Physics*, *390*, 51–65.

Leung, A. W., Varanyuwatana, P., & Halestrap, A. P. (2008). The mitochondrial phosphate carrier interacts with cyclophilin D and may play a key role in the permeability transition. *Journal of Biological Chemistry*, *283*(39), 26312–26323.

Lim, B. C., Lee, S., Shin, J.-Y., Kim, J.-I., Hwang, H., Kim, K. J., Hwang, Y. S., Seo, J.-S., & Chae, J. H. (2011). Genetic diagnosis of Duchenne and Becker muscular dystrophy using next-generation sequencing technology: Comprehensive mutational search in a single platform. *Journal of Medical Genetics*, *48*(11), 731–736.

Ling, X., Zhou, Y., Li, S.-W., Yan, B., & Wen, L. (2010). Modulation of mitochondrial permeability transition pore affects multidrug resistance in human hepatocellular carcinoma cells. *International Journal of Biological Sciences*, *6*(7), 773.

Liu, H., & Beckenbach, A. T. (1992). Evolution of the mitochondrial cytochrome oxidase II gene among 10 orders of insects. *Molecular Phylogenetics and Evolution*, *1*(1), 41–52.

Lockshin, R. A., & Zakeri, Z. (2004). Apoptosis, autophagy, and more. *The International Journal of Biochemistry & Cell Biology*, *36*(12), 2405–2419.

Mukherjee, P. K., Sahoo, A. K., Narayanan, N., Kumar, N. S., & Ponnusankar, S. (2009). Lead finding from medicinal plants with hepatoprotective potentials. *Expert Opinion on Drug Discovery*, *4*(5), 545–576.

Neginskaya, M. A., Solesio, M. E., Berezhnaya, E. V., Amodeo, G. F., Mnatsakanyan, N., Jonas, E. A., & Pavlov, E. V. (2019). ATP synthase C-subunit-deficient mitochondria have a small cyclosporine A-sensitive channel, but lack the permeability transition pore. *Cell Reports*, *26*(1), 11–17.

Newmeyer, D. D., Farschon, D. M., & Reed, J. C. (1994). Cell-free apoptosis in Xenopus egg extracts: Inhibition by Bcl-2 and requirement for an organelle fraction enriched in mitochondria. *Cell*, *79*(2), 353–364.

Nicholls, d. g. (1974). The influence of respiration and ATP hydrolysis on the proton-electrochemical gradient across the inner membrane of rat-liver mitochondria as determined by ion distribution. *European Journal of Biochemistry*, *50*(1), 305–315.

Olorunsogo, O. O., & Malomo, S. O. (1984). Mitochondrial bioenergetics during exposure of rats to perfluidone, a fluorinated arylalkylsulphonamide. *Chemico-Biological Interactions*, *52*(1), 67–78.

Park, S. W., Kim, M., Kim, M., D'Agati, V. D., & Lee, H. T. (2011). Sphingosine kinase 1 protects against renal ischemia–reperfusion injury in mice by sphingosine-1-phosphate1 receptor activation. *Kidney International*, *80*(12), 1315–1327.

Parrinello, M., & Rahman, A. (1981). Polymorphic transitions in single crystals: A new molecular dynamics method. *Journal of Applied Physics*, *52*(12), 7182–7190.

Patra, A., Jha, S., Murthy, P. N., Vaibhav, A. D., Chattopadhyay, P., Panigrahi, G., & Roy, D. (2009). Anti-inflammatory and antipyretic activities of Hygrophila spinosa T. Anders leaves (Acanthaceae). *Tropical Journal of Pharmaceutical Research*, *8*(2).

Petronilli, V., Miotto, G., Canton, M., Brini, M., Colonna, R., Bernardi, P., & Di Lisa, F. (1999). Transient and long-lasting openings of the mitochondrial permeability transition pore can be monitored directly in intact cells by changes in mitochondrial calcein fluorescence. *Biophysical Journal*, *76*(2), 725–734.

Schardt, D. (2008). Manipulating mitochondria. *Nutrition Action Health Letter*, *35*(10), 810.

Schinzel, A. C., Takeuchi, O., Huang, Z., Fisher, J. K., Zhou, Z., Rubens, J., Hetz, C., Danial, N. N., Moskowitz, M. A., & Korsmeyer, S. J. (2005). Cyclophilin D is a component of mitochondrial permeability transition and mediates neuronal cell death after focal cerebral ischemia. *Proceedings of the National Academy of Sciences*, *102*(34), 12005–12010.

Schüttelkopf, A. W., & Van Aalten, D. M. (2004). PRODRG: a tool for high-throughput crystallography of protein–ligand complexes. *Acta Crystallographica Section D: Biological Crystallography*, *60*(8), 1355–1363.

Seddek, A. latif S., Mahmoud, M. E., Shiina, T., Hirayama, H., Iwami, M., Miyazawa, S., Nikami, H., Takewaki, T., & Shimizu, Y. (2009). Extract from Calotropis procera latex activates murine macrophages. *Journal of Natural Medicines*, *63*, 297–303.

Sousa, S. F., Fernandes, P. A., & Ramos, M. J. (2006). Protein–ligand docking: Current status and future challenges. *Proteins: Structure, Function, and Bioinformatics*, *65*(1), 15–26.

Sun, S.-Y., Hail Jr, N., & Lotan, R. (2004). Apoptosis as a novel target for cancer chemoprevention. *Journal of the National Cancer Institute*, *96*(9), 662–672.

Tarasov, A. I., Griffiths, E. J., & Rutter, G. A. (2012). Regulation of ATP production by mitochondrial Ca2+. *Cell Calcium*, *52*(1), 28–35.

Uchino, H., Minamikawa-Tachino, R., Kristián, T., Perkins, G., Narazaki, M., Siesjö, B. K., & Shibasaki, F. (2002). Differential neuroprotection by cyclosporin A and FK506 following ischemia corresponds with differing abilities to inhibit calcineurin and the mitochondrial permeability transition. *Neurobiology of Disease*, *10*(3), 219–233.

Walsh, C., Zydowsky, L., & McKeon, F. D. (1992). Cyclosporin A, the cyclophilin class of peptidylprolyl isomerases, and blockade of T cell signal transduction. *Journal of Biological Chemistry*, *267*(19), 13115–13118.

Warne, J., Pryce, G., Hill, J. M., Shi, X., Lennerås, F., Puentes, F., Kip, M., Hilditch, L., Walker, P., & Simone, M. I. (2016). Selective inhibition of the mitochondrial permeability transition pore protects against neurodegeneration in experimental multiple sclerosis. *Journal of Biological Chemistry*, *291*(9), 4356–4373.

Yang, W.-H., Ding, C.-K. C., Sun, T., Rupprecht, G., Lin, C.-C., Hsu, D., & Chi, J.-T. (2019). The hippo pathway effector TAZ regulates ferroptosis in renal cell carcinoma. *Cell Reports*, *28*(10), 2501–2508.

Zhang, L., He, D., Li, K., Liu, H., Wang, B., Zheng, L., & Li, J. (2017). Emodin targets mitochondrial cyclophilin D to induce apoptosis in HepG2 cells. *Biomedicine & Pharmacotherapy*, *90*, 222–228.

Zoratti, M., & Szabò, I. (1995). The mitochondrial permeability transition. *Biochimica et Biophysica Acta (BBA)-Reviews on Biomembranes*, *1241*(2), 139–176.